SPECTROSCOPIC STUDY OF METAL VAPOR KINETICS

A. Macek, et al

Atlantic Research Corporation

Prepared for:

Advanced Research Projects Agency
Rome Air Development Center

April 1974

UNCLASSIFIED

SECURITY CLASSIFICATION OF THIS PAGE (When Data Entered)

AD 783 275

REPORT DOCUMENTATION PAGE

READ INSTRUCTIONS BEFORE COMPLETING FORM

1. REPORT NUMBER: RADC-TR-74-184	2. GOVT ACCESSION NO.
3. RECIPIENT'S CATALOG NUMBER	
4. TITLE (and Subtitle): Spectroscopic Study of Metal Vapor Kinetics	5. TYPE OF REPORT & PERIOD COVERED: Technical Report, May 1973 - April 1974
6. PERFORMING ORG. REPORT NUMBER: N/A	
7. AUTHOR(s): A. Maček, P. J. Goede, R. S. Scheffee and P. Zukovich	8. CONTRACT OR GRANT NUMBER(s): F30602-73-C-0313
9. PERFORMING ORGANIZATION NAME AND ADDRESS: Atlantic Research Corporation, 5390 Cherokee Avenue, Alexandria VA 22314	10. PROGRAM ELEMENT, PROJECT, TASK AREA & WORK UNIT NUMBERS: 62301E, 16490208
11. CONTROLLING OFFICE NAME AND ADDRESS: Defense Advanced Research Projects Agency, 1400 Wilson Blvd, Arlington VA 22209	12. REPORT DATE: April 1974
	13. NUMBER OF PAGES: ~~47~~ 56
14. MONITORING AGENCY NAME & ADDRESS (if different from Controlling Office): Rome Air Development Center (OCSE), ATTN: Joseph J. Simons, Griffiss AFB NY 13441	15. SECURITY CLASS. (of this report): UNCLASSIFIED
	15a. DECLASSIFICATION/DOWNGRADING SCHEDULE

16. DISTRIBUTION STATEMENT (of this Report)

Approved for public release, distribution unlimited.

17. DISTRIBUTION STATEMENT (of the abstract entered in Block 20, if different from Report)

Approved for public release, distribution unlimited.

18. SUPPLEMENTARY NOTES

Monitored by RADC (Joseph J. Simons)
Griffiss AFB NY 13441

19. KEY WORDS (Continue on reverse side if necessary and identify by block number)

Spectroscopy
Aluminum Releases
Iron Releases

20. ABSTRACT (Continue on reverse side if necessary and identify by block number)

This report presents the results of a theoretical and laboratory study involving the formulation and evaluation of pyrotechnic mixtures for aluminum and iron vapors. Various mixtures of tungstic oxide, zirconium, with Al, Fe or Fe_2O_3 powders were mixed into different proportions pressed into strands, and burned at subatmospheric pressure. The mixture performance was judged by (a) qualitative observations of the plumes recorded by a movie camera; (b) burning time and (c) quantitative absorption spectroscopy of Al and Fe vapors. As a result, measurements, in a high altitude simulation tank, using tungstic

DD FORM 1 JAN 73 1473 EDITION OF 1 NOV 65 IS OBSOLETE

oxide, zirconium and aluminum in a pressed strand configuration, indicate a release efficiency of the order of 10 to 20%.

SPECTROSCOPIC STUDY OF METAL VAPOR KINETICS

A. Maček
P. J. Goede
R. S. Scheffee
P. P. Zukovich

Contractor: Atlantic Research Corporation
Contract Number: F30602-73-C-0313
Effective Date of Contract: 29 May 1973
Contract Expiration Date: 1 April 1974
Amount of Contract: $54,940.00
Program Code Number: 3E20

Principal Investigator: Dr. Andrej Macek
Phone: 202 354-3400

Project Engineer: Joseph J. Simons
Phone: 315 330-3055

This research was supported by the Defense Advanced Research Projects Agency of the Department of Defense and was monitored by Joseph J. Simons RADC (OCSE) GAFB NY 13441 under Contract F30602-73-C-0313, Job Order No. 16490208.

ib

This report has been reviewed by the Office of Information, RADC, and approved for release to the National Technical Information Service (NTIS).

This report has been reviewed and is approved.

TABLE OF CONTENTS

LIST OF ILLUSTRATIONS

I. GENERAL DESCRIPTION OF THE EXPERIMENTAL PROGRAM

The purpose of this project was the formulation and evaluation of pyrotechnic mixtures for release of aluminum and iron vapors. The starting point for the formulations was the previously described mixture of tungstic oxide, WO_3, and zirconium metal (1). When mixed in proportions stoichiometric to ZrO_2 and metallic W (67% WO_3, 37% Zr by weight), these two ingredients give very hot (> 3000°K) largely condensed products.

In the program which is the subject of the present report, WO_3, Zr, Al, Fe, and Fe_2O_3 powders were mixed in different proportions, pressed into strands with masses of 15 to 25 gm, and burned mostly at subatmospheric pressure. This type of release is based on the fact that metallic Al (or Fe) is the most volatile component among the flame products of any given formulation, so the product gas will consist predominantly of Al (or Fe) vapor; the detailed thermodynamics is discussed in Section II. The performance of the mixtures was judged by (a) qualitative observation of the plumes recorded by a movie camera; (b) burning-time, hence average linear burning-rate, measurement; and (c) quantitative absorption spectroscopy of Al and Fe vapors. Details of the two absorption-spectroscopy methods used are presented in Section III.

The experimental program consisted of three parts. In the first part, twelve preliminary tests were made, six each with aluminum and iron, in which rough burning rates were obtained by visual observation of total burning times over the pressure range of 10 torr to 1 atm. These tests were made at the Atlantic Research Corporation Pine Ridge facility in a small vacuum tank without any elaborate instrumentation.

The second part, comprising a large portion of the entire experimental program, consisted of 30 tests with aluminum, 14 with iron, and 6 blank ones (WO_3 and Zr mixed in different proportions), at pressures ranging from 60μ Hg to 100 torr. These tests were conducted in the main high-altitude chamber at Atlantic Research. The chamber is a cylinder 1.83m in diameter, 7.62m long. The experimental arrangement is shown in Fig. 1. A 30-cm diameter tube, placed coaxially in the center of the high-altitude chamber, contained a protective flow of argon. The pyrotechnic strands were pressed to about 4gm/cc into aluminum or steel tubes 1.3 cm in diameter, 6.4 cm long and placed at the downstream end of the 30-cm tube. Absorption-spectroscopy

traverses were made at downstream distances from the strand varying from x = 1.9 cm to x = 7.6 cm (1.5 to 6 strand diameters), and lateral distances from y = 0 to y = 7.6 cm. In addition to the spectrometric measurements, color movies were taken of all releases, usually at 64fps.

The third part of the program consisted of two releases of pure aluminum vapor, made by a thermal vaporization technique described in Ref. 2. This technique allows generation of quantitatively known metal-vapor streams (temperature, pressure, mass-flow). The releases were made at the relatively high pressure of 15 torr for the purpose of calibration of the continuum-source absorption-spectroscopy measurements (see Section III). The experimental arrangement was quite similar to that shown in Fig. 1, the orifice of the thermal vaporizer taking place of the downstream end of the strand. Optical traverses were made at x = 1.9 cm, y = 0.

II. THERMODYNAMIC COMPUTATIONS

Several series of thermodynamic computations of flame products and temperatures were made for mixtures consisting of WO_3, Zr, Mg, Al, Fe, and Fe_2O_3. In all cases the necessary computer input data were taken from JANNAF Thermochemical Tables.

1. Aluminum-Containing Formulations

As discussed in more detail in Ref. 1, in the pressure range of 1 torr to 1 atm stoichiometric mixtures of WO_3 and Zr undergo flame reactions closely approximated by the equation:

$$2WO_3(s) + 3Zr(s) \rightarrow 3ZrO_2(l) + 2W(l \text{ or } s),\ 3000\ K < T_F < 4000°K$$

Dissociative vaporization of $ZrO_2(l)$ into ZrO(g) and $ZrO_2(g)$ is favored by low pressures; hence the large dependence of T_F on pressure. However, the extent of vaporization is always small.

Addition of aluminum to the WO_3/Zr system gives rise to Al(g) as virtually the only additional flame product, because the free energies of the zirconium oxides and aluminum oxides are such that aluminum remains largely reduced. Progressive addition of aluminum thus keeps improving the efficiency of Al(g) generation until the temperature drops to the point where aluminum begins to condense.

Results of full thermodynamic computations for 4.8 and 9.1% Al by weight (5 and 10 parts of Al added to 100 parts of the WO_3/Zr mixture) are given in Table I. For 13.0% Al the computer predicts condensation of the metal. The computations were made at pressures of 10 torr and 100 torr, because estimates of aluminum vapor flow dynamics indicate that the probable pressure inside the strand tube will be in that range (see Section V-1). Inspection of Table I shows that $Al_2O(g)$ is the only aluminum compound of any importance; its formation is favored by high pressure and by high content of aluminum in the formulation.

In view of these computations, we chose three aluminum-containing compositions for experimental work; all of them had the stoichiometric ratio of WO_3/Zr (63/37 by weight), and the amounts of aluminum were 8, 12 and 16% by weight.

2. Iron-Containing Formulations

Thermodynamic computations were made for WO_3/Zr/Fe mixtures analogous to the kind made for aluminum (Section II-1). The results are quite similar when one takes into account the two obvious differences: a higher atomic weight and a lower volability for iron.

Many variations of the above-described approach, i.e. a WO_3/Zr mixture loaded with iron powder, are possible. Table II gives a set of thermodynamic computations illustrating a few of these. Since full thermodynamic computations of all such compositions predict only a small degree of formation of suboxides (e.g., FeO, ZrO, AlO -- compare Table I), the calculations in Table II were made on the assumption that the only products are: Fe(g), Fe(l), W(s), ZrO_2(s), Al_2O_3(l) and MgO(l). These approximate calculations are entirely adequate for our purpose here.

Inspection of Table II leads to four interesting conclusions. First, iron may be introduced not only in metallic form (formulations 1A, 1B, 1C), but also as Fe_2O_3 (2A through 3C). Second, the reducing metal need not be zirconium, but can also be magnesium (1B, 2B, 3B) or aluminum (1C, 2C, 3C). Third, if iron is introduced as Fe_2O_3, the amounts of WO_3 can be varied over a wide range, and can even be equal to zero (2A, 2B, 2C). Finally, it is clearly seen that on the weight basis magnesium is always the best reducing metal, followed by zirconium, and then aluminum.

All three zirconium-containing formulations, 1A, 2A and 3A of Table II, were prepared and evaluated experimentally.

III. MEASUREMENTS OF METAL-ATOM NUMBER DENSITIES

Densities of metal atoms in release plumes were determined optically from combined extinction and emission measurements. For the experimental release configurations employed, a hollow-cathode source was appropriate for measurements of number densities less than about 10^{13}/cc, while a continuum source was appropriate for measurements of number densities greater than about 10^{15} - 10^{16}/cc.

1. Apparent Absorption Measurements

The apparent absorption produced by an atomic absorption line in a release plume was measured using the technique and apparatus described below.* Number densities were then determined from the apparent absorption measurements by considering line broadening, curve-of-growth and instrumental broadening effects.

a. Optical Absorption Apparatus

The optical apparatus utilized for the apparent absorption measurements is shown schematically in Figure 2. Both emission and extinction measurements are made so that an extinction measurement may be corrected for the effect of plume emission. Similarly, measurements are made at both the absorption line wavelength and a neighboring wavelength so that a gas absorption measurement may be corrected for the effect of particle extinction.

Three types of light sources were employed. Standard Westinghouse hollow-cathode lamps were utilized for measuring low atom densities. The hollow-cathode sources were especially useful for determining if any appreciable concentrations of atomic metals were being generated. For high densities, either a General Electric tungsten strip lamp or a Sylvania Zr source was used. All three types of light sources were powered by direct current power supplies to avoid undesirable modulation of the lamp radiation.

*Apparent absorption is defined in terms of the power detected at the exit slit plane of a monochromator and thus includes the spectral effects produced by the light source and monochromator, as well as the true absorption.

The radiation from a light source was mechanically chopped, focused on a release plume inside the high-altitude chamber (Fig. 1), divided into two nearly equal intensity beams and focused on the entrance slits of two SPEX Industries monochromators. The radiant power transmitted through a monochromator exit slit was detected using an EMI photomultiplier tube (PMT), amplified using a Keithley picoammeter (PAM) and recorded on both a Consolidated Electronics Corporation visicorder and a Tektronix dual beam storage oscilloscope. Quartz refractive optics or aluminized reflective optics were employed throughout to extend the spectral coverage to ultraviolet absorption lines.

b. Analysis of Measurement Technique

For the purpose of optically evaluating plume number densities it is assumed that the flow from a release device may be characterized as a one-dimensional flow. While the effects of plume transverse density gradients produced by expansion and mixing with ambient gases are not considered in this simplified approach, the first order density effects should be reasonably accounted for. The equation of radiative transfer may therefore be written as

$$N_\nu(s_2) = N_\nu(s_1)\ \mathrm{EXP}\ [-K_\nu(s_2 - s_1)] + \int_{s_1}^{s_2} j_\nu\ \mathrm{EXP}\ [K_\nu(s-s_2)]\ ds \qquad (1)$$

where

N_ν = spectral radiance (w/cm^2 sr hz)

(s_1, s_2) = plume optical path (cm)

K_ν = volumetric extinction coefficient (cm^{-1})

j_ν = volumetric emission coefficient (w/cm^3 sr hz)

The power detected at the exit slit of a monochromator is computed by assuming that the entrance slit is uniformly illuminated by a narrow cone of rays

$$P_D = T_R A_{ENS} \Omega_{ENS} \int_{-\infty}^{\infty}\int_{-\infty}^{\infty} N_\nu(s_2)\, g|\nu' - \nu| h(\nu')\, d\nu d\nu' , \qquad (2)$$

where

P_D = power detected at the exit slit (w)

T_R = transmission of the receiver optics between the plume and the monochromator entrance slit

A_{ENS} = area of the entrance slit (cm^2)

Ω_{ENS} = solid angle of the illumination cone of rays at the entrance slit (sr)

ν = frequency of incident radiation (hz)

ν' = position in the exit slit plane of a monochromator corresponding to the frequency ν for an infinitely narrow entrance slit, perfect monochromator optics and no diffraction effects (hz),

For the wide slit widths employed, the slit function g is square

$$g|\nu' - \nu| = \begin{cases} g_o & |\nu' - \nu| < \Delta\nu_{ENS}/2 \\ 0 & \text{otherwise} \end{cases} \qquad (3)$$

where g_o is a constant and

$\Delta\nu_{ENS}$ = apparent bandpass of entrance slit (hz)

= linear dispersion x entrance slit width.

The exit slit response is also square

$$h(\nu') = \begin{cases} 1 & |\nu' - \nu_o'| < \Delta\nu'_{EXS}/2 \\ 0 & \text{otherwise} \end{cases} \qquad (4)$$

where

ν_o' = center position of exit slit (hz)

$\Delta\nu'_{EXS}$ = apparent bandpass of exit slit (hz)

= linear dispersion x exit slit width.

For the small solid angles subtended by the source optics at the plume ($\sim 4 \times 10^{-3}$ sr), the volumetric emission coefficient will not be strongly influenced by scattering of source radiation, so the apparent plume transmission is defined by

$$T = \frac{P_D^{S+F} - P_D^F}{P_D^S} \quad , \tag{5}$$

where

T = apparent plume transmission

P_D^{S+F} = power detected when the light source is viewed through the plume (w)

P_D^F = power detected when the plume is viewed alone (w)

P_D^S = power detected when the light source is viewed without the plume (w).

T may be written as

$$T = \frac{\int_{-\infty}^{\infty}\int_{-\infty}^{\infty} N_\nu(s_1)\,\mathrm{EXP}\,[-K_\nu(s_2-s_1)]\,g\,|\nu' - \nu|\,h(\nu')\,d\nu d\nu'}{\int_{-\infty}^{\infty}\int_{-\infty}^{\infty} N_\nu(s_1)\,g\,|\nu' - \nu|\,h(\nu')\,d\nu d\nu'} \tag{6}$$

The relevant radiative interaction processes occuring in the plume are emission, absorption and scattering by hot particles and emission and absorption by gases. To separate the gas and particle effects, measurements are made both at an atomic absorption line and at a neighboring frequency. The volumetric extinction coefficients may therefore be written as

$$K_\nu(\nu_L) = K_\nu^{GA}(\nu_L) + K_\nu^{P}(\nu_L) \tag{7}$$

$$K_\nu(\nu_C) = K_\nu^{P}(\nu_C), \tag{8}$$

where

ν_L = atomic absorption line frequency (hz)

ν_C = neighboring frequency (hz)

K_ν^{GA} = gas volumetric absorption coefficient (cm^{-1})

K_ν^{P} = particle volumetric extinction coefficient (cm^{-1}).

If ν_L and ν_C are sufficiently close, a gray-body behavior describes the particle spectral extinction

$$K_\nu^{P}(\nu_L) \simeq K_\nu^{P}(\nu_C) \tag{9}$$

The apparent gas absorption is defined by

$$A = 1 - \frac{T(\nu_L)}{T(\nu_C)} \tag{10}$$

It may be evaluated experimentally using Equations (5) and (10) as

$$A = 1 - \frac{\dfrac{P_D^{S+F}(\nu_L) - P_D^{F}(\nu_L)}{P_D^{S}(\nu_L)}}{\dfrac{P_D^{S+F}(\nu_C) - P_D^{F}(\nu_C)}{P_D^{S}(\nu_C)}} \tag{11}$$

It may also be evaluated theoretically using Equations (6) - (10) as

$$A = \frac{\int_{-\infty}^{\infty}\int_{-\infty}^{\infty} N_\nu(s_1)\{1 - EXP\,[-K_\nu^{GA}(s_2-s_1)]\}g\,|\nu'-\nu|h(\nu')\,d\nu d\nu'}{\int_{-\infty}^{\infty}\int_{-\infty}^{\infty} N_\nu(s_1)g\,|\nu'-\nu|h(\nu')\,d\nu d\nu'} \tag{12}$$

To interpret the apparent gas absorption in turns of atom number densities, it will first be necessary to consider the line broadening processes.

2. Absorption Line Broadening

The spectral gas absorption coefficient, K_ν^{GA}, may be written in terms of a normalized line shape factor as

$$K_\nu^{GA} = S(\nu)K \tag{13}$$

where

$S(\nu)$ = normalized line shape factor (hz^{-1})

K = integrated gas absorption coefficient (hz/cm)

The line shape factor is normalized to unity

$$\int_{-\infty}^{\infty} S(\nu)\,d\nu = 1 \tag{14}$$

The integrated gas absorption coefficient may be written in terms of the absorption oscillator strength for an electronic transition as

$$K \simeq \frac{\pi e^2}{m_e c} N_\ell f_{\ell u} \qquad (15)$$

where

e = electronic charge = 1.601×10^{-19} coulomb

m_e = electronic mass = 9.1083×10^{-28} gm

c = vacuum velocity of light = 2.99793×10^{10} cm/sec

N_ℓ = atom number density of lower energy level (cm^{-3})

$f_{\ell u}$ = absorption oscillator strength

Local thermodynamic equilibrium is assumed to hold so that

$$\frac{N_\ell}{N} = \frac{g_\ell \, EXP\ (-E_\ell/kT)}{\sum_i g_i \, EXP(-E_i/kT)} \qquad (16)$$

where

N = total atom number density (cm^{-3})

g_i = degeneracy of level i

E_i = energy of level i

k = Boltzmann's constant = 1.3804×10^{-23} j/°K

T = temperature (°K)

Natural, Doppler, Stark, resonance and van der Waals broadening were examined with regard to their influence on atom number density determinations. For the hollow cathode source method it was found that only Doppler broadening was important. For the continuum source method it was found that only natural, resonance and possibly van der Waals broadening were important. Van der Waals broadening was not included in the analysis of the continuum source method; however, it should be given further consideration in future work.

For the hollow cathode source method the line shape factor is Gaussian:

$$S(\nu) = \frac{1}{\gamma_D/2} \left(\frac{\ell n 2}{\pi}\right)^{\frac{1}{2}} \text{EXP}\left[-\ln 2 \left(\frac{\nu-\nu_o}{\gamma_D/2}\right)^2\right], \tag{17}$$

where

γ_D = Doppler line width (hz)*

$$= 2\nu_o \left(\frac{2\,k\,T\,\ell n 2}{mc^2}\right)^{\frac{1}{2}} \tag{18}$$

ν_o = line center frequency (hz)

m = atom mass (gm).

For the continuum source method the line shape factor is Lorenzian

$$S(\nu) = \frac{\gamma}{2\pi} \frac{1}{(\nu-\nu_o)^2 + (\gamma/2)^2}, \tag{19}$$

where

γ = line width (hz)

$$= \gamma_N + \gamma_R \tag{20}$$

γ_N = natural line width (hz)

γ_R = resonance line width (hz)

For a transition between a lower level ℓ and an upper level u the natural line width is

$$\gamma_N = \sum_{\ell'} A_{u\ell'} + \sum_{\ell'} A_{\ell\ell'} \tag{21}$$

where

$A_{u\ell}$ = Einstein coefficient for spontaneous emission (sec^{-1}).

The effects of resonance broadening are accurately described by an impact theory near the line center when

$$|\nu - \nu_o| \ll \frac{1}{2\pi \langle \tau_{CD} \rangle}, \tag{22}$$

where

$\langle \tau_{CD} \rangle$ = mean time of collision duration (sec).

Resonance broadening is accurately described by a static theory far from

* All line widths in this discussion pertain to the full width at half maximum.

the line center when

$$|\nu - \nu_o| \gg \frac{1}{2\pi \langle \tau_{CD} \rangle} \tag{23}$$

For the continuum source method the line profile far from the line center is the pertinent factor. It can be demonstrated, however, that the difference between the line shape factors predicted by an impact theory and a static theory are small far from the line center. For example, for

$$|\nu - \nu_o| \gg \gamma \tag{24}$$

$$\frac{[S(\nu)]_{AGIT}}{[S(\nu)]_{NNST}} \simeq 0.918 \left(\frac{g_\ell}{g_u}\right)^{\frac{1}{2}} \nu_i \tag{25}$$

where

$[S(\nu)]_{AGIT}$ = line shape factor predicted by the Ali-Griem impact theory (hz^{-1}) (Ref. 1,2)

$[S(\nu)]_{NNST}$ = line shape factor predicted by the nearest neighbor static theory (hz^{-1}) (Ref. 3)

Therefore the Ali-Griem impact theory predicts a line shape that is accurate for any reasonable distance from the line center. The resonance line width predicted by this theory is

$$\gamma_R = 0.306 \left(\frac{g_\ell}{g_u}\right)^{\frac{1}{2}} \frac{e^2 f_{\ell u} N}{m_e \nu_o} \tag{26}$$

3. Hollow-Cathode Method

For the hollow cathode sources and slit widths employed

$$\gamma^S \ll \Delta\nu_{ENS}, \Delta\nu_{EXS} \tag{27}$$

where

γ^S = emission line width of source (hz)

The apparent absorption as represented by Equation (12) may therefore be simplified to

$$A \simeq \frac{\int_{-\infty}^{\infty}\int_{-\infty}^{\infty} N_\nu(s_1)\,\{1-\mathrm{EXP}[-K_\nu^{GA}(s_2-s_1)]\}\,d\nu}{\int_{-\infty}^{\infty}\int_{-\infty}^{\infty} N_\nu(s_1)\,d\nu} \tag{28}$$

It is further assumed that a hollow cathode emission line is Doppler-broadened at the translational temperature of the source

$$N_\nu(s_1) = \frac{N^S(s_1)}{\gamma^S/2}\left(\frac{\ell n 2}{\pi}\right)^{\frac{1}{2}} \mathrm{EXP}\left[-\ell n 2\left(\frac{\nu-\nu_o}{\gamma^S/2}\right)^2\right] \tag{29}$$

where

$N^S(s_1)$ = source integrated radiance ($w/cm^2 sr$)

$$\gamma^S = 2\nu_o\left(\frac{2kT^T \ell n 2}{mc^2}\right)^{\frac{1}{2}} \tag{30}$$

T^T = translational temperature of the source (°K)

For the follow cathode sources used in the measurements it was estimated that the translational temperature of the source was 300°K.

Setting

$$\alpha = \gamma^S/\gamma_D \tag{31}$$

and

$$\omega = \sqrt{\ell n 2}\left(\frac{\nu-\nu_o}{\gamma_D/2}\right) \tag{32}$$

Equation (28) may be rewritten as

$$A = \frac{\int_{-\infty}^{\infty} \mathrm{EXP}\,(-\omega^2/\alpha^2)\,\{1-\mathrm{EXP}\,[-C'\,\mathrm{EXP}\,(-\omega^2)]\}d\omega}{\int_{-\infty}^{\infty}\mathrm{EXP}\,(-\omega^2/\alpha^2)\,d\omega} \tag{33}$$

where

$$C' = \frac{K^{GA}(s_2-s_1)}{\gamma_D/2}\left(\frac{\ell n 2}{\pi}\right)^{\frac{1}{2}} \tag{34}$$

Mitchell and Zemansky (Ref. 4) have evaluated Equation (33) using the series expansion

$$A = \frac{C'}{\sqrt{1+\alpha^2}} - \frac{(C')^2}{2!\sqrt{1+2\alpha^2}} + \cdots + \frac{(-1)^{n+1}(C')^n}{n!\sqrt{1+n\alpha^2}} + \cdots \quad (35)$$

The atom number density is then computed from the expression

$$N = \frac{m_e c C' \nu_D}{2 (\pi \ell n 2)^{\frac{1}{2}} e^2 (N_\ell/N) f_{\ell u} (s_2 - s_1)} \quad (36)$$

It is particularly pertinent to consider that case where the hollow cathode source is nearly 100 percent absorbed since this occurs at relatively low atom number densities. For the purposes of this work, nearly 100 percent absorption is taken to be 97 percent or greater absorption since the experimental records could not be read more accurately than to within about ± 3 percent. For A = 0.97 and T = 1000°K it is found from Equation (35) that C' = 4.8. Absorption oscillator strengths and Einstein A coefficients were obtained from Wiese et, al. (Ref. 5, 6), where possible, and from Corliss and Bozman (Ref. 7) otherwise. The state degeneracies were obtained from Moore (Ref. 8). For a pathlength of 2.5 cm, a number density of 3.52×10^{12}/cc is computed for the 3961 Å aluminum line, while 5.68×10^{12}/cc is computed for the 3917 Å iron line.

4. Continuum Source Method

For the continuum source and small slit widths employed, Equation (12) may be simplified to

$$A = \frac{\int_{-\infty}^{\infty}\int_{-\infty}^{\infty} [1-\mathrm{EXP}\ [-K_\nu^{GA}(s_2-s_1)]]\ g\,|\nu' - \nu|\ h(\nu')\,d\nu d\nu'}{\int_{-\infty}^{\infty}\int_{-\infty}^{\infty} g\ |\nu'-\nu\ |h(\nu')\,d\nu d\nu'} \quad (37)$$

This expression was evaluated numerically on an IBM/370 computer from the expression

$$A = 1 - \frac{1}{2\, y_{ENS} y_{EXS}} \int_0^{y_{EXS}} f(y)\, dy \tag{38}$$

where

$$y_{ENS} = \Delta\nu_{ENS}/\nu \tag{39}$$

$$y_{EXS} = \Delta\nu_{EXS}/\nu \tag{40}$$

$$f(y) = f(x)\Big|_{y-y_{ENS}}^{y+y_{ENS}} \tag{41}$$

$$f(x) = x\ \mathrm{EXP}\ (-C_3/x^2) - \frac{x}{|x|}\sqrt{\pi C_3}\ \ \mathrm{ERFC}\ \left(\frac{\sqrt{C_3}}{|x|}\right) \tag{42}$$

$$C_3 = \frac{2K^{GA}\,(s_2 - s_1)}{\pi\nu} \tag{43}$$

Typical results are shown in Figures 1.2 and 1.3 for the aluminum 3961 Å line and the iron 3719 Å line, respectively.

5. Conclusions Regarding Number Density Measurements

Based on the results obtained, the hollow cathode source method is appropriate for measurements of atom number densities less than about 10^{13}/cc, while the continuum source method is appropriate for densities greater than about 10^{15} - 10^{16}/cc.

It is recommended that future work include a more accurate plume model than one-dimensional flow and that van der Waals broadening be further evaluated with regard to its impact on the continuum source measurements.

IV. TESTING PROGRAM

1. Preliminary Tests

The preliminary series consisted of six tests with the WO_3/Zr/Al (58/34/8) mixture, and six tests with WO_3/Zr/Fe(55/32/13). The mixtures were pressed into phenolic tubes at 20,000 psi compression. The purpose of this series was to obtain general information about the pressed strands: physical characteristics, ignitability, burning rates, and the effects of particle size variation.

The tungstic anhydride was in powdered form, screened through a No. 325-mesh screen. Microscopic inspection revealed fairly uniform particle sizes, with diameters ranging mostly from 30 to 40μm. The material was found satisfactory in the preliminary tests and was used throughout the program.

Two grades of zirconium were used. One sample was a relatively coarse powder, with particle diameters ranging widely from about 5 to 50μm. The other sample had a smaller average size, about 10μm, with particles ranging from about 3 to 20μm. These two powders will be referred to as "coarse" and "fine" respectively.

The aluminum powder consisted of spherical particles having quite uniform diameters of about 3μm. This very fine powder was found easy to handle, it pressed well into the strands, and gave reproducible burning rates. Since small particles are obviously desirable for metal vaporization, we continued to use this powder in these and all subsequent tests.

The iron powder had nominal particle diameters of 50μm. While this material gave satisfactory results in this preliminary series of tests, it was suspected that the particle sizes were too large for efficient vaporization. Testing in the high-altitude facility (Section IV 2b) confirmed the suspicion.

a. Ignition

Strands made with fine zirconium powder were found to ignite more easily than strands with coarse zirconium. However, since fine zirconium powder has a bad safety record, we developed a method which allows reliable ignition also for strands made with coarse zirconium. The strand geometry, with the ignition system developed in the preliminary testing program, is shown in Fig. 5. This geometry was used in

all subsequent tests (Section IV 2). The tube into which the strands were pressed was made of aluminum, 0.34 or 0.16 cm wall thickness, for aluminum releases, and steel (about 0.3 cm wall) for iron releases. The length of the main charge (coarse zirconium) varied from test to test from 4.7 to 5.8 cm.

b. Burning Rates

Average strand burning rates were obtained by measurement of total burning times (Table III). These burning times are only approximate -- indeed, they give the lower limit of true rates, because the measurement includes also the ignition time, which is small but not negligible; more accurate burning rates will be given in Section IV 2. Nevertheless, the measurements allow several pertinent observations.

First, the strands burn well down to pressures of 10 torr. Indeed, these preliminary data suggested (and subsequent more accurate work confirmed) that at such low pressures the burning rate is independent of pressure; this is a very important point, because it means that the releases will be operative under arbitrarily low pressures, hence at arbitrarily high altitudes. Second, mixtures with fine zirconium burn faster than mixtures with coarse zirconium. Third, at sufficiently high pressures, the burning rate does become a function of pressure.

2. Instrumented Tests in the High-Altitude Facility

The instrumented tests in the Atlantic Research high-altitude facility were run as shown in Fig. 1 (see Section I).

Three series of tests were run with aluminum. All three were formulated with the stoichiometric WO_3/Zr(63.0/37.0) mixture, to which aluminum powder was added in amounts such that total percentages of aluminum were 8, 12 and 16.

The iron tests also consisted of three series. In one of them, iron powder was added to the stoichiometric WO_3/Zr mixture, as in the case of aluminum. In the second series, Fe_2O_3 powder was added to a WO_3/Zr mixture. The third series was made with a binary Fe_2O_3/Zr formulation. Both Fe_2O_3 mixtures were formulated so that the theoretical flame temperatures of all three iron series were equal (see Table II).

In addition to the tests in which aluminum or iron was included in the

pyrotechnic formulation, we made a series of blank runs to observe the appearance of the basic mixture without a volatile metal. Three fuel-rich WO_3/Zr mixtures were tested.

The Al-containing, the Fe-containing and the blank runs will now be described under separate headings. All the formulations were burned in the geometry shown schematically in Fig. 5.

A word of explanation about the general methodology will be useful before a description of the individual tests. As demonstrated in detail in Section III, the continuum-source method for the metal-vapor density measurements, which was being developed during these tests, is useful only for number densities of the order of 10^{16}/cc or greater. At temperatures of about 2000°K, this lower limit corresponds to a partial pressure of about 2 torr. However, we found in the early experiments with the continuum-source method that at total pressures exceeding about 1 torr, the emission from incandescent particles in the release plume (ZrO_2, W) interfered with the absorption measurements. Therefore, as the experimental program progressed, our efforts with the continuum-source method were directed toward: (a) higher pressures, hence higher total gas densities; (b) smaller distances x and y from the strand orifice (see Fig. 1), where there is less mixing with argon and therefore higher partial pressures of Al(g) and Fe(g); (c) high-temperature continuum sources to overcome the continuum emission. On the other hand, the more conventional hollow-cathode method for density measurements is useful only up to number densities of the order of 10^{13}/cc, hence metal vapor partial pressures in the μHg range. Our efforts with the hollow-cathode technique therefore were directed toward (a) low ambient pressures (low total densities), and (b) large values of x and y (low partial pressures of Al(g) and Fe(g) due to mixing). Inspection of Tables IV through VIII will show these trends.

a. Aluminum Releases

The experimental conditions and the results of the strand burnings with the WO_3/Zr/Al formulations, mixed in proportions (58.0/34.0/8.0), (55.4/32.6/12.0) and (52.9/31.1/16.0), are collected in Tables IV, V, and VI respectively.

The headings of the columns in Tables IV through VIII are mostly self-explanatory. Color movies at either 32 or 64 fps were taken of all tests. The column headed "Burning Rate - Camera" gives an average linear burning rate

calculated from the burning time as recorded by the movie camera. Comparison of that column in Table IV with the data in Table III shows that burning rates in Table IV correspond to shorter burning times. This is so, because in most tests the slow-motion pictures give a clear distinction between the ignition phase and the combustion of the aluminized portion of the strand. Typically, the entire ignition system, including the WO_3/Zr pellet made with fine zirconium (see Fig. 5), burns in 0.05 to 0.1 sec. The subsequent combustion of the release strand characterized by a large, intensely luminous plume takes 1 to 2 seconds, depending on the length and formulation of the strand. Table III data do not discriminate between the ignition and the combustion phases, and ascribe the total luminous time to the release strands; hence the low burning rates in that table.

In addition to the camera burning rates, many -- but not all -- absorption spectrograms give a quantitative measure of Al(g) and Fe(g) release duration. If there is emission from plumes, the duration of burning can be sometimes obtained also from the emission trace of the spectroscopic record. Burning rates obtained in this way are listed in a separate column in Tables IV - VIII ("Spec. rec."), and they usually agree approximately with the camera records. While generally less reliable, they are especially useful in the few cases, where the interpretation of the movies is not obvious.

The column headed "Absorption" means preferential absorption of the Al-line channel (3961Å). The control channel in runs with aluminum was centered on the 3521Å neon line in the hollow-cathode runs, and on the 4000Å wavelength in the continuum-source runs.

We now proceed to the description of the individual tests, starting with Table IV.

Runs 2 and 3 in Table IV differ from the rest of the aluminum runs in that they were made with fine zirconium powder. In agreement with the trend suggested by the preliminary tests (Table III), these strands burned somewhat faster than the rest.

All the absorption records in Table IV obtained with the hollow cathode source show saturation absorption. This includes Test T4, which was run under the conditions of extreme attenuation of Al vapor: 100μHg total pressure, and the absorption beam location 6 strand diameters (d) downstream and 6d off axis.

Tests of the series 1A through 5A were run with the tungsten strip lamp at 32 amp, corresponding to a brightness temperature of about 1950°K. The downstream location of the absorption beam was 7.6 cm = 6d in all tests. The chamber pressures in this series were 1.4±0.2 torr. The series shows that the continuum emission from the plume is manageable, providing the spectroscopic traverse is made at $y \geq 3.8$ cm = 3d. In run 3A, y = 2d, the continuum emission was sufficiently strong to drive the active (3961Å) beam off the records of the visicorder and the oscilloscope. Thus, strictly speaking, we do not know whether there was any preferential absorption of the active channel in this run. However, in the context of the rest of Tables IV, V and VI, preferential absorption in run 3A appears very unlikely.

In view of the results of tests 1A - 5A, two more tests were run at about the same chamber pressure, but with on-axis (y = 0) traverses and increased lamp temperatures. T1 at 38 amp corresponding to about 2180°K and T2 at 46 amp, corresponding to an estimated 2400-2450°K (temperature beyond the calibration range). Run T1 showed some emission, on both the active and the control channel, and run T2 some attenuation, all within the range of the recording instruments. Neither run gave evidence of preferential absorption of the active channel.

In runs D1 and D2 the strip lamp was replaced by a 300-watt Sylvania zirconium-arc source having an estimated brightness temperature of 3000 - 3100°K, and the absorption traverse was made directly downstream (y = 0) at x = 1.5 d. Strong emission was observed in both runs. However, in run D1 at the chamber pressure of 20 torr, the emission stayed within the range of the recording instruments, and a small preferential absorption of about 6% was observed for a portion of the run duration. In run D2, at 100 torr, very strong emission drove both beams out of the instrumental range throughout the duration of the run. Thus no conclusion can be reached about absorption in run D2.

Tests of the "T" series (T1 - T4 in Table IV, T5 - T8 in Table V, T9 - T12 in Table VI) were run with a slightly different experimental arrangement from the rest: they were fitted with a side-arm near the upstream end of the strand. The side-arm contained a strain-gauge, intended to measure the pressure inside the strand tube during combustion. The strain-gauge data gave no useful information, so they will not be discussed. The presence of the side-arm had no appreciable effect on the plume appearance and the spectroscopic measurement for most of the duration of

the experiment, but in some runs it caused an uncertainty in the determination of the burning time; hence some erratic burning rates among the "T" series runs. The explanation is not difficult. Toward the end of the run, as the burning front reaches the side-arm, the product gases find a temporary outlet into the dead space between the strand and the gauge, causing a perturbation of the plume downstream of the strand tube. All absorption records of the "T" series show a "dent" toward the end of run, which does not appear to affect the total length of the record. However, the camera records show that in some runs the visible plume does not recover well after the interruption, making the determination of the burning time difficult. Thus in the "T" series, the absorption records sometimes appear to give more reliable burning rates than the camera.

Tests with 12% aluminum (Table V) generally confirm the trends established with 8% formulations. The hollow-cathode runs, T7 and T8, show 100% absorption, as in the equivalent 8% Al tests. Runs with the tungsten strip lamp show that at pressures of the order of 1 torr and a location 6d directly downstream of the strand, the continuum emission from the plume can be overcome by high lamp temperature (in run T6 the estimated lamp brightness temperature was between 2500 and 2600°K). However, the Al(g) number density was below the value needed to give readable absorption. Runs D3 and D4 show that at high pressures, 19 and 100 torr respectively, and a location 1.5d downstream of the strand, even the Zr-arc source has too low a temperature to overcome the plume emission. Thus the question of Al(g) number densities under these conditions remains unresolved.

The main characteristic of the 16% Al experiments (Table VI) is that their combustion was rather poor. First, one of the strands (T12) failed to ignite. Second, two strands (5B and T9) burned slowly and erratically with poorly defined plumes. Third, most of the movies showed large luminous drops emerging from the strand tube. This was probably molten aluminum, indicating inefficient vaporization. Spectroscopic diagnosis of the plumes gave the results characteristic of most other tests: 100% absorption with the hollow cathode, and no absorption with the continuum sources.

Two general conclusions can be made regarding the use of WO_3/Zr/Al strands. First, the pressing of strands gives reproducible densities: the average values are 4.00 gm/cc for 8% Al, 3.92 gm/cc for 12% Al, and 3.75 gm/cc for 16% Al, with probable errors of $\pm$0.02 to 0.05 gm/cc. These densities correspond to about

2/3 of the average crystal density of the ingredients; thus the samples were quite porous. Second, the burning rates of the strands are quite reproducible. The apparent irregularities of burning rates in Tables IV, V and VI (camera rates) are readily accounted for by the difference in geometry of the "T" series tests, described earlier. Even in that series, an inspection of the data obtained by both the camera and the spectroscopy leads to the conclusion that the true rate will always be about 3 cm/sec. The only exception is run T10; this run was made with the 16% Al formulation which we know tends to burn erratically. The best average value of the burning rate (with coarse zirconium) is 3.3 cm/sec with a probably error of about $\pm$0.1 cm/sec.

b. Iron Releases

The headings of Tables VI and VII, documenting the iron releases, are the same as the headings of Tables IV - VI, described in Section IV 2a. The active absorption channel in the iron tests was centered on the Fe 3720Å line. The control channel was centered on the Ne 3521Å.

Three pairs of runs were made with the WO_3/Zr/Fe (54.8/33.1/13.1) mixtures. The data are collected in Table VII. Samples A1 and A2 were hand-tamped into steel tubes, so the density was only about 40% of the average crystal density of the ingredients. Samples M1 and M2 were pressed to somewhat higher densities. Samples B1 and B2 were pressed at 20,000 psi to pressures in excess of 4 gm/cc; the porosity of these highly pressed samples was roughly the same as in the aluminum-containing samples. There is indication that the high-density strands burned somewhat better, but combustion of all the samples in Table VIIwas generally poor, giving weak, ill-defined plumes, and probably ejecting unvaporized iron particles. Run M1 at a relatively high pressure of 2 torr and with a central (y = 0) absorption traverse showed preferential Fe(g) absorption in excess of the saturation number density. Other runs at pressures of the order of 0.1 torr and with off-axis traverses also showed high percentages of absorption, but sometimes falling a little short of 100%.

Tests in which iron was introduced into the formulation in the form of Fe_2O_3 are summarized in Table VIII. Both formulations -- WO_3/Zr/Fe_2O_3(31.6/41.6/26.8) and Zr/Fe_2O_3(46.1/53.9) -- burned well and generated strong, well-defined gaseous plumes; the average burning rates for the two formulations are 2.6 and 3.2 cm/sec respectively. The first five strands in Table VIII were prepared in the same way

(20,000 psi), and they all had the same relative density, about 65% of the crystal value. The last two samples were pressed to a lower density, ca. 40% of the crystal.

The spectroscopic results are similar to those given in Table VII. The two runs at 2 torr gave hollow-cathode beam absorption clearly in excess of the saturation level. The two runs at 110μHg with off-axis traverses gave absorption levels higher than 97%, possibly 100%, since records normally can be read only in the range from about 3% to 97%. Run IV-4, at 60μHg, showed 50±10% over the first second of the run. Thereafter, there was attenuation of both the active and the control channel throughout the run (burning time 1.84 sec), and for 1-2 sec after the run. The 5 torr Zr-arc run at x = 1.5 d, y = 0, gave no evidence of absorption.

c. Blank Runs

In addition to strands which contained either aluminum or iron, six strands were prepared with three different binary WO_3/Zr mixtures: 60/40, 45/55, and 30/70. All these are more fuel-rich than the stoichiometric 63/37 mixture which served as the basis for most other formulations. The purpose of these series was to observe the appearance of "releases" without a volatile metal.It must be pointed out that only the very fuel-rich WO_3/Zr(30/70) formulation has the theoretical flame temperature approximating the flame temperatures of the Al and Fe-containing formulations, which have much less excess metal fuel. The reason, of course, is that Al and Fe vaporize, thus creating a very large heat sink, while excess zirconium does not.

The powdered mixtures were found to press well into strands having reproducible densities. However, their combustion appeared erratic, and there was no well-defined plume such as we had observed in the case of formulations with Al and Fe_2O_3 powders. The visible products consisted largely of low-velocity incandescent particles. The appearance of the blank strands resembled somewhat the appearance of the strands made with 13% of large iron powder, which also gave poor combustion results (Table VII). Comparison of these tests with the tests of Tables IV, V, VI and VIII indicates clearly that the observed well-developed plumes (Al and Fe_2O_3 formulations) are due to the volatile metals.

d. Analysis of Combustion Residues

All the strands burned in such a way that very substantial solid residues

were left inside the strand tubes after combustion. The overall dimensions of the residues were about the same as those of original strands. Thus it appears that, as the burning front proceeded upstream, the volatile combustion products filtered continuously through a solid porous bed, entraining some loose particles, probably largely from the downstream end of the strand.

Some of the residues were found to be fused firmly to the walls of the tubes, and could not be dislodged. In other cases, however, the residue could be removed in one piece. Masses of the solid residues ranged widely from 44 to 85% of the original mass of the sample. The weight data on the residues are collected in Table IX.

Three of the residues listed in Table IX were analyzed for total aluminum: T4 (8% Al in the original formulation); T5 (12% Al); and T9 (16% Al). The samples were washed in a large excess of hot NaOH to dissolve the aluminum species and the solutions analyzed by atomic absorption. The weight percentages of total aluminum in the three samples were 1.69 (T4), 0.43 (T5), and 1.94 (T9). Expressed in a somewhat different way, 14.9% of the original aluminum in T4 was found in the residue, hence 85.1% had been in the plume; in T5 the partition was 2.5% in the residue and 97.5% in the plume; and in T9, 7.0% in the residue, 93.0% in the plume.

e. Calibration of the Continuum Method by Controlled Al Vapor Releases

Controlled jets of pure aluminum vapor were released in the high altitude facility at 15 torr. The purpose was to generate streams of Al(g) having high number densities of Al atoms, in excess of 10^{16}/cc, which would be sufficient to give measurable absorption of the Al 3961Å by the continuum-technique method.

Two runs were made in which aluminum was released by the metal-vaporization technique developed at Atlantic Research under a previous RADC contract (Ref. 2). In each run, a 500mg high-purity aluminum sample was placed into a tungsten-lined cavity inside a graphite heater. The heater was brought to a temperature above 2000°K within a few seconds. The entire sample was vaporized at a temperature of about 2200°K within 9 sec, i.e. at an average rate of about 60mg/sec. The heater was provided with an orifice, 0.64 cm in diameter. As explained in Ref. 2, vaporization of aluminum under these conditions leads to a choked-flow jet of the metal vapor. The estimated pressure inside the vaporizer cavity was about 30 torr.

The geometry of these calibration experiments was very similar to that used

in evaluating the aluminum-containing and iron-containing strands, because the heater was placed at the usual location of the strands (see Fig. 1). A narrow, strongly luminous jet emerged from the orifice over the duration of the run. Absorption beam traverses were made directly downstream of the orifice: $x = 3d = 1.9$ cm, $y = 0$.

A tungsten strip lamp was used as a source of continuum radiation in both runs. In the first run, the lamp was run at 31.5 amp, corresponding to about 1930°K brightness temperature. Strong preferential emission of the 3961Å line drove the active beam off the range of the recording instruments, so no absorption measurement could be made. In the second run, the lamp current was increased to 38 amp, corresponding to about 2180°K. Preferential absorption of the 3961Å line was observed for 6 sec, i.e. over two thirds of the visually observed duration of the run. The absorption level was varying between 10 and 13%.

V. DISCUSSION

1. Estimates of Gas Flow in the Strand Tube

We shall now make an approximate estimate of pressures and gas flows which can be expected at the mouth of the strand tube during the combustion of aluminum and iron releases.

We take first the case of a $WO_3/Zr/Al$ formulation containing 8% aluminum. The total mass of a typical release is about 25 gm (see Table I), i.e., 2 gm of aluminum. The typical burning time of the strand, 5 cm long, 1.3 cm in diameter, is 1.5 sec. Thus the average mass-flow rate $\dot{m}_{Al} = 1.3$ gm/sec. We now make the assumption that all of the aluminum is vaporized during the combustion of the strand, and that aluminum vapor is the only gas in the products. The temperature of Al-gas at the mouth of the strand-tube will be

$$T = \frac{T_{flame}}{1 + \frac{\gamma-1}{2}} = \frac{2600}{1.33} = 1955°K$$

At sufficiently low ambient (vacuum-tank) pressures the flow will be sonic. At 1955°K, the sound velocity in the aluminum vapor is $c = 1.00 \times 10^5$ cm/sec. The two relations

$$P = \frac{\rho}{M} RT,$$

where ρ is density and M the atomic weight of the vapor, and

$$\dot{m} = \rho Ac,$$

where A is the cross-sectional area of the strand tube, determine the pressure at the exit plane of the strand tube. Substitution of the appropriate values gives a throat pressure of 46 torr for the 8% Al strands. Thus, if the release does vaporize the aluminum efficiently, the flow should choke at 46 torr ambient pressure. Below that pressure, the conditions inside the strand tube should be independent of the ambient. In particular, one should expect the burning rate to be independent of the ambient pressure. Our experimental results are roughly consistent with that picture. There is ample documentation (see Table IV) that burning rates of the

strands do not change in the range of ambient pressures from 100μHg to 1.6 torr. The burning rate data at 20 torr and 100 torr are also in the same range of values, but these are single points, which would have to verified before any firm conclusions can be drawn. The approximate data of Table III suggest that the burning rate becomes independent of the ambient conditions at a pressure between 10 and 100 torr.

When the above flow calculations are repeated with typical Fe-strand values (23 gm total strand, 13% iron, $\dot{m}_{Fe}$ = 1.2 gm/sec), the theoretical choking pressure turns out to be 30 torr, i.e., somewhat lower than for aluminum. This result calls for a further consideration. The 30-torr "throat" pressure corresponds to a 61 torr "chamber" pressure, i.e., pressure at the surface of the strand inside the tube. However, 61 torr is in excess of the vapor pressure of iron at 2600°K, which is only 41 torr. Thus, theoretically, 30 torr ambient would cause condensation of iron. Efficient releases of iron should be expected only at ambient pressures, ca. 20 torr or lower. As discussed in Section IV 2 c, our releases with iron powder gave poor plumes so the measured strand burning rates are questionable. The releases in which iron was introduced into the formulation as Fe_2O_3 are too few for a firm conclusion, but it certainly appears that their burning rates are independent of pressure from 60μHg to at least 2 torr, possibly 5 torr. Thus, it appears reasonable to suppose that the flow chokes at pressures exceeding 5 torr.

2. Spectroscopic Measurement of Metal Vapor Densities

a. Aluminum

The spectroscopic continuum-absorption method was calibrated under experimental conditions which allow a reasonable analysis of these data (see Section IV 2 d). The ambient pressure was 15 torr. The estimated temperature inside the vaporizer was about 2200°K, corresponding to about 30 torr: thus the expansion ratio of the Al-vapor jet was about 2, i.e., the flow was near critical. Since the orifice diameter was 0.64 cm, we estimate the diameter of the jet to have been about 0.7 cm. According to Fig. 3, the measured apparent absorption in the calibration run, 10 to 13%, corresponds to Al number densities of 3 to 4 x 10^{16}/cc.

An independent estimate of the actual Al-density in the optical beam can also be made, because the traverse was made across the center of the jet, only three diameters downstream of the orifice. Thus mixing with argon could be neglected. The estimated temperature of the jet, after expansion from the vaporizer, is about 1700°K.

At 15 torr, the corresponding number density of aluminum is 9×10^{16}/cc.

The agreement within a factor of 2 to 3 between an a priori calculation of line-broadening and the estimate of the actual Al number density is in itself satisfactory. However, there are two considerations which indicate that in a more accurately designed experiment, the agreement would be even closer. First, the geometry of the intersection of the optical beam with the metal-vapor jet was not ideal, because the optical beam, 9mm diameter, was somewhat larger than the estimated jet diameter. If the jet were wider, or the beam narrower, one should expect a larger apparent absorption.

Second, it must be noted that the estimated jet temperature, 1700°K, is below the condensation temperature of aluminum, which is about 2100°K at 15 torr. Thus, one must consider the possibility of partial condensation of the metal in the jet, which would again cause a lower measurement of the apparent absorption. Actually, the fact that the measured optical absorption is of the correct order of magnitude can be taken as evidence that no substantial condensation occurred upstream of the optical beam. While we have not addressed the problem of condensation of aluminum, the persistence of supersaturation for about 20μsec (travel time from the vaporizer to the optical beam) at the rather low pressure of 15 torr does not appear unreasonable.

The only strand-release test which gave a measurable continuum-source absorption reading is D1, Table IV, which was run at 20 torr ambient pressure. Only rough, order-of-magnitude estimates of the Al-vapor flow are possible from the data in this test. The 6% apparent absorption corresponds to a number density between 1×10^{16} and 3×10^{16}, depending on whether one uses the a priori calculation (Fig. 3) or the experimental calibration (see above). If we assume that the strand flame temperature had the thermodynamically predicted value, 2600°K, then the pressure at the strand surface inside the tube was 92 torr (see Section V 1), the ratio of the flame pressure to the ambient was 4.6, and the flow across the optical beam was supersonic (M = 1.6). The equation of continuity then gives Al-vapor mass-flow rates of 0.1 to 0.3 gm/sec. This compares to a value of about 1 gm/sec for the total aluminum flow, obtained from the burning-rate data. However, since there is no assurance that the adiabatic flame temperature was attained, it is more conservative to assume merely that the flow velocity was roughly sonic; this would be true even

at lower flame temperatures and much more modest flame pressures. The Al(g) mass-flow rates calculated from the point densities of 1×10^{16}/cc and 3×10^{16}/cc then would be 0.07 and 0.2 gm/sec, corresponding to 7% and 20% vaporization efficiencies respectively.

The hollow-cathode measurements cannot be used for a quantitative determination of the Al(g) release rates, because the apparent absorption was 100% in all runs, including the extreme case of run T4, where the Al(g) density was expected to be lower than in any other run. The ambient pressure in T4 was 100μHg, corresponding to a total number density of the order of 10^{15}/cc. The absorption measurement in that run was made in an area far downstream and to the side of the release (x = 6d, y = 6d) where extensive mixing should be expected. We know that very high expansion pressure ratios were involved in tests at such low ambient pressures, probably more than 100. However, a much better controlled experiment would be needed to give a reasonable quantitative estimate of plume expansion and mixing under these conditions. Thus the available absorption measurements do not lend themselves to an estimate of even the lower limit of the release efficiency. The point-density measurement in run T4 was probably somewhat below 10^{13}/cc (see Section III 3, keeping in mind that the optical path length is not known for a traverse far off the main axis of the plume). This means that the average mole fraction of Al(g) in the optical beam was of the order of 0.01 or larger. Since extensive mixing no doubt took place, it appears quite likely that the Al(g) number densities in the unmixed portions of the plume were of the order of total species number densities.

b. Iron

No absorption results were obtained with the continuum-source method. This is not surprising, because tests were run only up to 5 torr ambient pressure.

Results of the hollow-cathode tests are similar to those obtained with aluminum releases. Inspection of Tables VII and VIII shows that in some cases the absorption level appeared to be slightly below 100%, whereas with aluminum the hollow-cathode records always indicated absorption clearly in excess of the saturation level. There are two possible reasons for this difference: first, the fact that 100% absorption with the Fe-3521Å line corresponds to a higher absorber density than with the Al-3961Å line; and second that Fe-vapor densities

in fact were lower. In either case, the rough, order-of-magnitude estimate for the densities obtained by the hollow-cathode method with aluminum (Section V a) apply also to iron. The fact that the test run at the lowest pressure (run III-3, 60μHg) gave substantially less absorption than any other may appear suggestive. However, there are several runs at pressures of about $100_{\mu}H_g$ which give about 100% absorption. Since a modest decrease of pressure from 100μHg to 60μHg should not be expected to give a large decrease of Fe(g) density (see Fig. 4), no special significance should be attached to this single run.

VI. CONCLUSIONS

1. Pressed pyrotechnic mixtures developed and used in this project present a simple and convenient method for upper-atmosphere releases of aluminum and iron vapors. Compression of the mixtures at moderate pressures (20,000 psi) gives reproducible densities and reproducible linear burning rates in the range of 2 to 4 cm/sec. At ambient pressures below about 10 torr the burning rates are independent of pressure. Thus the releases can be used at arbitrary altitudes.

2. Tungstic oxide (WO_3) particle diameters of about 40 to 50μm are satisfactory for both aluminum and iron releases.

Small-particle zirconium powder, ca. 10μm average diameter, is also satisfactory from the viewpoint of release performance. However, since this material is known to be hazardous to handle, coarser zirconium is preferable. The recommended ignition method for formulations containing coarse zirconium has been detailed in this report.

Very fine ($\bar{d}$ = 3μm) spherical aluminum powder used in this program is recommended for any further work. Iron powder of similar quality does not appear to be available. Coarse iron powder ($\bar{d} \sim 50\mu m$) is not satisfactory. Commercial iron oxide powder (NAPCO "red"), having a wide distribution of particle sizes ($9 m^2/gm$ area), gives good reproducible combustion results.

3. Thermodynamic computations show that formulations for iron vapor releases in which magnesium is substituted for zirconium give higher theoretical yields of Fe(g). Since magnesium may also be safer to handle than zirconium, experimental evaluation of magnesium-containing mixtures is recommended.

4. On the basis of the currently available information, obtained under this contract, we recommend formulations with 12% of aluminum and about 18% of iron in the form of Fe_2O_3 (see Table II) for the two respective releases. Further tests with larger amounts of iron are recommended.

5. An experimental determination of the continuum-absorption method for the 3961Å Al line has been obtained, which is in satisfactory agreement with the *a priori* calculation of the resonance-broadening process. The Al number densities must be in excess of 10^{16}/cc for experimental measurement across path lengths of the order of 1cm. The contribution of van der Waals broadening may become significant at these pressures, and it

should be studied.

Measurement of the Al(g) density for a formulation containing 8% aluminum by the continuum-absorption method indicated a release efficiency of the order of 10 to 20% of the theoretical. More testing is needed to verify this number.

Since the hollow-cathode absorption technique is useful only for number densities of the order of 5×10^{12}/cc or less, there is a large range of densities which are inaccessible to the currently available absorption-spectroscopy methods. Plume-modeling and a better design for experimental plume generation (shaped nozzles) will be required, if the low densities measurable by the hollow-cathode technique are to be used for quantitative determination of Al(g) and Fe(g) release efficiencies.

REFERENCES

1. This reference available to qualified military and government agencies on request from RADC (OCSE) Griffiss AFB NY 13441.

2. A. Maček, Metal Oxidation in a Vacuum Tank. RADC-TR-73-281, July 1973.

3. A. W. Ali and H. R. Griem, "Theory of Resonance Broadening of Spectral Lines by Atom-Atom Impacts," Physical Review, 140, 4A, A1044-A1049, 1965.

4. A. W. Ali and H. R. Griem, "Errata for Theory of Resonance Broadening of Spectral Lines by Atom-Atom Impacts," Physical Review, 144, 366, 1966.

5. W. Lochte-Holtgreven, Plasma Diagnostics, Wiley Interscience, 1968, pp.81-82.

6. A. C. G. Mitchell and M. W. Zemansky, Resonance Radiation and Excited Atoms, Cambridge University Press, 1971, p. 323.

7. W. L. Wiese, M. W. Smith and B. M. Glennon, Atomic Transition Probabilities, Volume I, Hydrogen Through Neon, NSRDS-NBS-4, 1966.

8. W. L. Wiese, M. W. Smith and B. M. Miles, Atomic Transition Probabilities, Volume II, Sodium Through Calcium, NSRDS-NBS-22, 1969.

9. C. H. Corliss and W. R. Bozman, Experimental Transition Probabilities for Spectral Lines of Seventy Elements, NBS Monograph 53, 1962.

10. C. E. Moore, Atomic Energy Levels, Volumes I, II, III, Circular of the NBS 467, 1949, 1952 and 1958.

TABLE I. THERMODYNAMIC COMPUTATIONS OF ALUMINUM-CONTAINING COMPOSITIONS

COMPOSITION (GRAMS): WO_3/Zr/Al (63/37/X)

PRODUCTS (moles)	X = 5 gm Al		X = 10 gm Al	
	10 torr	100 torr	10 torr	100 torr
Al (g)	0.166	0.164	0.348	0.290
Al_2O (g)	0.008	0.011	0.011	0.040
AlO (g)	0.003	0.001	–	–
ZrO_2 (l)	0.396	0.398	–	–
ZrO_2 (s)	–	–	0.401	0.387
ZrO (g)	0.008	0.007	0.001	0.001
ZrO_2 (g)	0.001	–	–	–
Zr (l)	–	–	0.003	0.018
W (s)	0.272	0.272	0.272	0.272
FLAME T (°K)	3026	3086	2426	2585

SPECIES INCLUDED IN THE COMPUTATION AND FOUND TO BE ABSENT ($\leq$ 0.0005 mole): WO_2 (g), W_3O_8 (g), WO_2 (s), W (g), WO_3 (g), W_3O_9 (g), WO_3 (s), W (l), WO (g), W_2O_6 (g), W_4O_{12} (g), W (s), Zr (g), Al (s), Al_2O_3 (l), Al_2O_2 (g), Al_2O_3 (s), AlO_2 (g), Al (l), O_2 (g), O (g).

TABLE II. IRON-RELEASE CALCULATIONS

FORMULATION NO.	Fe	Fe_2O_3	Al	Mg	Zr	WO_3	Fe(g) YIELD WEIGHT %
1A	13.0				32.2	54.8	13.0
1B	17.2			19.8		63.0	17.2
1C	12.6		16.5			70.9	12.6
2A		53.9			46.1		17.7
2B		68.6		31.4			26.7
2C		74.7	25.3				15.5
3A		26.8			41.6	31.6	18.7
3B		38.4		28.1		33.5	26.8
3C		25.3	21.0			53.7	17.7

THEORETICAL FLAME TEMPERATURE OF ALL FORMULATIONS ARBITRARILY CHOSEN TO BE 2600°K. AT THAT TEMPERATURE, THE VAPOR PRESSURE OF IRON IS 41 torr.

TABLE III. APPROXIMATE BURNING RATE MEASUREMENTS[a] (cm/sec) (WO_3/Zr/Al and WO_3/Zr/Fe)

	PRESSURE (torr)		
	10	100	760
Al STRANDS - COARSE Zr	2.6	3.1	3.6
Al STRANDS - FINE Zr	3.1	–	–
Fe STRANDS - COARSE Zr	0.8	1.0	1.2
Fe STRANDS - FINE Zr	1.3	–	–

[a]SEE TEXT FOR EXPLANATION WHY THESE RATES ARE ONLY APPROXIMATE.

TABLE IV. INSTRUMENTED STRAND TESTS – 8 PERCENT ALUMINUM.

RUN NO.	WEIGHT (gm)	DENSITY (gm/cc)	CHAMBER P (torr)	ABSORPTION SPECTROSCOPY			BURNING RATE (cm/sec)		ABSORPTION (percent)	COMMENT
				SOURCE[a]	LOCATION X (cm)	LOCATION Y (cm)	CAMERA	SPECTR. REC.		
2	19.22	3.78	0.24	HC	7.6	5.1	~5	4.2	100	FINE Zr POWDER
3	23.35	4.05	0.23	HC	7.6	5.1	4.1	4.1	100	FINE Zr POWDER
4	27.61	4.10	0.26	HC	7.6	5.1	3.3	3.3	100	
1A	26.33	4.05	1.6	WL 32	7.6	5.1	–	–	–	STRAND WET. INCOMPLETE ERRATIC COMBUSTION.
2A	23.79	3.96	1.2	WL 32	7.6	5.1	3.0	–	0	
3A	24.14	3.38	1.4	WL 32	7.6	2.5	3.0	~3	? (0)	EMISSION ON BOTH CHANNELS. ACTIVE CHANNEL PARTLY OFF RECORD.
4A	24.03	4.01	1.3	WL 32	7.6	3.8	3.0	–	0	SMALL ERRATIC EMISSION ON BOTH CHANNELS. NO CLEAR DEFINITION OF BURNING TIME FROM SPECTROSCOPY.
5A	24.29	4.05	1.5	WL 32	7.6	3.8	3.0	~3.1	0	SMALL EMISSION. POOR DEFINITION OF BURNING TIME.
T1	25.29	3.88	1.6	WL 38	7.6	0	?	1.3	0	SPECTROSCOPY RECORD SHOWS EMISSION. SEE TEXT FOR CAMERA RECORDS OF THE "T" SERIES.
T2	25.40	4.06	1.6	WL 46	7.6	0	3.5	~3.5	0	WEAK ATTENUATION ON BOTH CHANNELS: SPECTROSCOPIC BURNING TIME APPROXIMATE.
T3	25.38	3.93	0.10	HC	7.6	5.1	3.4	(2.5 - 5)	100	PARTIAL SPECTROSCOPIC RECORD: 100% ABSORPTION FOR A TIME 1 sec $< t_b <$ 2 sec.
T4	22.41	3.99	0.10	HC	7.6	7.6	3.5	3.5	100	
D1	25.02	4.04	20	Zr	1.9	0	2.8	(2-4)	6 ± 2	STRONG EMISSION ON BOTH CHANNELS, BUT NOT OFF THE RECORD. NO CLEARLY DEFINED BURN. TIME FROM SPECTROSCOPY (1.2 to 2.2 sec)
D2	24.61	3.98	100	Zr	1.9	0	3.2	2.6 ?	?	STRONG EMISSION - BOTH SPECTROSCOPIC CHANNELS OFF THE RECORD.

[a]HC: HOLLOW-CATHODE RADIATION SOURCE.
WL: TUNGSTEN STRIP LAMP; CURRENT INDICATED IN AMPS (e.g., 32 amps in Run 1A)
Zr: ZIRCONIUM ARC SOURCE.

TABLE V. TESTS WITH 12 PERCENT ALUMINUM.

RUN NO.	WEIGHT (gm)	DENSITY (gm/cc)	CHAMBER P (torr)	ABSORPTION SPECTROSCOPY			BURNING RATE (cm/sec)		ABSORPTION (percent)	COMMENT
				SOURCE[a]	LOCATION X (cm)	LOCATION Y (cm)	CAMERA	SPECTR. REC.		
T-5	24.35	3.89	1.6	WL 38	7.6	0	3.2	<4.1	0	PARTIAL SPECTROS. RECORD SHOWS RATHER STRONG EMISSION, ANO BURN TIME $>$ 1.2 sec
T-6	24.37	3.94	1.7	WL 49.5	7.6	0	4.8(?)	~ 3.9	0	WEAK EMISSION. APPROXIM. BURN TIME FROM SPECTROS. RECORO. SEE TEXT FOR CAMERA RECORDS OF THE "T" SERIES.
T-7	24.53	4.05	0.13	HC	7.6	5.1	5.0(?)	3.2	100	SPECTROS. RECORO SHOWS INTERRUPTION. SEE TEXT.
T-8	24.45	3.91	0.11	HC	7.6	7.6	5.2(?)	<3.3	100	PARTIAL SPECTROS. RECORO GIVES UPPER LIMIT OF BURN RATE.
D-3	25.35	3.85	19	Zr	1.9	0	3.8	3.8	?	EMISSION CAUSEO ABSORPTION BEAM TO GO OFF RECORO.
D-4	24.44	3.90	100	Zr	1.9	0	3.6	?	?	EMISSION CAUSEO ABSORPTION BEAM TO GO OFF RECORO.

[a]HC: HOLLOW-CATHOOE. WL: TUNGSTEN STRIP LAMP, CURRENT IN AMPS. Zr: ZIRCONIUM ARC SOURCE.

TABLE VI. TESTS WITH 16 PERCENT ALUMINUM.

RUN NO.	WEIGHT (gm)	DENSITY (gm/cc)	CHAMBER P (torr)	ABSORPTION SPECTROSCOPY			BURNING RATE (cm/sec)		ABSORPTION (percent)	COMMENT
				SOURCE[a]	LOCATION X (cm)	LOCATION Y (cm)	CAMERA	SPECTR. REC.		
18	22.96	3.75	2.0	HC	7.6	3.8	3.4	3.0	100	VIRTUALLY NO EMISSION ON EITHER CHANNEL NO ATTENUATION OF CONTROL CHANNEL
28	23.07	3.69	2.0	WL 32	7.6	3.8	3.5	~3.3	0	SOME ATTENUATION OF BOTH BEAMS. DUST DEPOSITION ON CHAMBER WINDOWS.
38	23.02	3.74	1.9	WL 32	7.6	2.5	3.3	–	0	NO EMISSION OR ATTENUATION OF EITHER CHANNEL
48	23.01	3.74	1.8	WL 32	0	1.3	3.2	–	0	SLIGHT ATTENUATION OF BOTH BEAMS.
58	22.90	3.78	0.14	HC	7.6	3.8	(~2.5)	(~1)	100	FAULTY BURN.
T9	24.39	3.75	2.0	WL 38	7.6	0	–	–	0	FAULTY BURN.
T10	24.47	3.76	1.7	WL 48	7.6	0	5.4	4.5-5.5	0	SEE TEXT.
T11	24.60	3.78	0.09	HC	7.6	5.1	5.5	> 3.4	100	IRREGULARITY IN ABSOR. RECORD, AS IN MOST "T" SEPIES RUNS. TOTAL ABSORPTION TIME < 1.5 sec
T12	24.53	3.77	0.09	HC	7.6	7.6	–	–	–	IGNITION FAILURE

[a]HC: HOLLOW CATHODE. WL: TUNGSTEN STRIP LAMP, CURRENT IN AMPS. Zr: ZIRCONIUM ARC SOURCE.

TABLE VII. TESTS WITH 13 PERCENT IRON POWDER.

RUN NO.	WEIGHT (gm)	OENSITY (gm/cc)	CHAMBER P (torr)	ABSORPTION SPECTROSCOPY			BURNING RATE (cm/sec)		ABSORPTION (percent)	COMMENT
				SOURCE[a]	LOCATION X (cm)	LOCATION Y (cm)	CAMERA	SPECTR. REC.		
A1	16.00	2.78	0.09	HC	7.6	5.1	1.3	~ 1.3	96	HANO-TAMPED SAMPLE, HENCE VERY LOW OENSITY. POOR BURN, POOR PLUME
A2	15.90	2.68	0.13	HC	7.6	5.1	1.4	–	> 97	VERY POOR BURN. HANO-TAMPEO SAMPLE. ABSORPTION >97% FOR FRACTION OF BURN ONLY.
M2	19.38	3.16	0.10	HC	7.6	5.1	1.2	< 1.5	> 97	LONG, WEAK BURN. POOR PLUME, APPARENTLY LARGELY PARTICLES.
M1	17.18	3.13	2.0	HC	7.6	0	1.7	–	100	POOR BURN. HOT PARTICLES.
B1	23.20	4.17	0.13	HC	7.6	5.1	2.3	~ 2	UP TO ~ 95	ERRATIC BURNING
B2	23.30	4.19	0.09	HC	7.6	5.1	2.0	~ 2	100	GOOO BURNING FOR 1.2 sec, ERRATIC BURNING FOR ABOUT ANOTHER SECONO.

[a]HC: HOLLOW-CATHODE SOURCE.

TABLE VIII. TESTS WITH Fe_2O_3 POWDER.

RUN NO.	WEIGHT (gm)	DENSITY (gm/cc)	CHAMBER P (torr)	ABSORPTION SPECTROSCOPY			BURNING RATE (cm/sec)		AB
				SOURCE[a]	LOCATION X (cm)	LOCATION Y (cm)	CAMERA	SPECTR. REC.	
III-1[b]	24.99	3.99	2.0	HC	7.6	0	2.6	2.9	
III-2	24.13	4.06	2.0	HC	7.6	0	2.5	~ 2.5	
III-3	24.95	4.01	0.06	HC	7.6	5.1	2.6	–	5
IV-4[c]	23.67	3.40	0.11	HC	7.6	5.1	3.3	~ 3.5	>
IV-5	24.94	3.37	0.11	HC	7.6	5.1	3.1	3-3.5	>
F-1	17.17	2.47	20	Zr	1.9	0	–	–	
F-2	17.30	2.46	5.0	Zr	1.9	0	3.2	–	

[a]HC: HOLLOW-CATHODE SOURCE. Zr: ZIRCONIUM ARC SOURCE.

[b]COMPOSITION OF SERIES III: $WO_3/Zr/Fe_2O_3$ (31.6/41.6/26.8)

[c]COMPOSITION OF SERIES IV AND SERIES F: Zr/Fe_2O_3 (46.1/53.9)

TABLE VIII. TESTS WITH Fe_2O_3 POWDER.

ABSORPTION SPECTHOSCOPY			BURNING RATE (cm/sec)		ABSORPTION (percent)	COMMENT
	LOCATION					
URCE[a]	X (cm)	Y (cm)	CAMERA	SPECTR. REC.		
C	7.6	0	2.6	2.9	100	STRONG EMISSION ON BOTH CHANNELS.
C	7.6	0	2.5	~ 2.5	100	EMISSION ON BOTH CHANNELS.
C	7.6	5.1	2.6	–	50 ± 10	ATTENUATION OF BOTH BEAMS AFTER BURN. DUST IN CHAMBER OR ON WINDOW (?)
C	7.6	5.1	3.3	~ 3.5	> 97	CLEAR CONTROL CHANNEL.
C	7.6	5.1	3.1	3-3.5	> 97	
r	1.9	0	–	–	–	MISFIRE
r	1.9	0	3.2	–	0	VIRTUALLY NO ATTENUATION OR EMISSION ON EITHER CHANNEL.

IRCONIUM ARC SOURCE.

/41.6/26.8)

$_2O_3$ (46.1/53.9)

TABLE VIII. TESTS WITH Fe_2O_3 POWDER.

RUN NO.	WEIGHT (gm)	OENSITY (gm/cc)	CHAMBER P (torr)	ABSORPTION SPECTROSCOPY			BURNING RATE (cm/sec)		ABSORPTION (percent)	COMMENT
				SOURCE[a]	LOCATION X (cm)	LOCATION Y (cm)	CAMERA	SPECTR. REC.		
III-1[b]	24.99	3.99	2.0	HC	7.6	0	2.6	2.9	100	STRONG EMISSION ON BOTH CHANNELS.
III-2	24.13	4.06	2.0	HC	7.6	0	2.5	~2.5	100	EMISSION ON BOTH CHANNELS.
III-3	24.95	4.01	0.06	HC	7.6	5.1	2.6	–	50 ± 10	ATTENUATION OF BOTH BEAMS AFTER BURN. DUST IN CHAMBER OR ON WINDOW (?)
IV-4[c]	23.67	3.40	0.11	HC	7.6	5.1	3.3	~3.5	>97	CLEAR CONTROL CHANNEL.
IV-5	24.94	3.37	0.11	HC	7.6	5.1	3.1	3-3.5	>97	
F-1	17.17	2.47	20	Zr	1.9	0	–	–	–	MISFIRE
F-2	17.30	2.46	5.0	Zr	1.9	0	3.2	–	0	VIRTUALLY NO ATTENUATION OR EMISSION ON EITHER CHANNEL.

[a]HC: HOLLOW-CATHOOE SOURCE. Zr: ZIRCONIUM ARC SOURCE.

[b]COMPOSITION OF SERIES III: $WO_3/Zr/Fe_2O_3$ (31.6/41.6/26.8)

[c]COMPOSITION OF SERIES IV AND SERIES F: Zr/Fe_2O_3 (46.1/53.9)

FIGURE 1. EXPERIMENTAL ARRANGEMENT IN THE HIGH-ALTITUDE FACILITY.

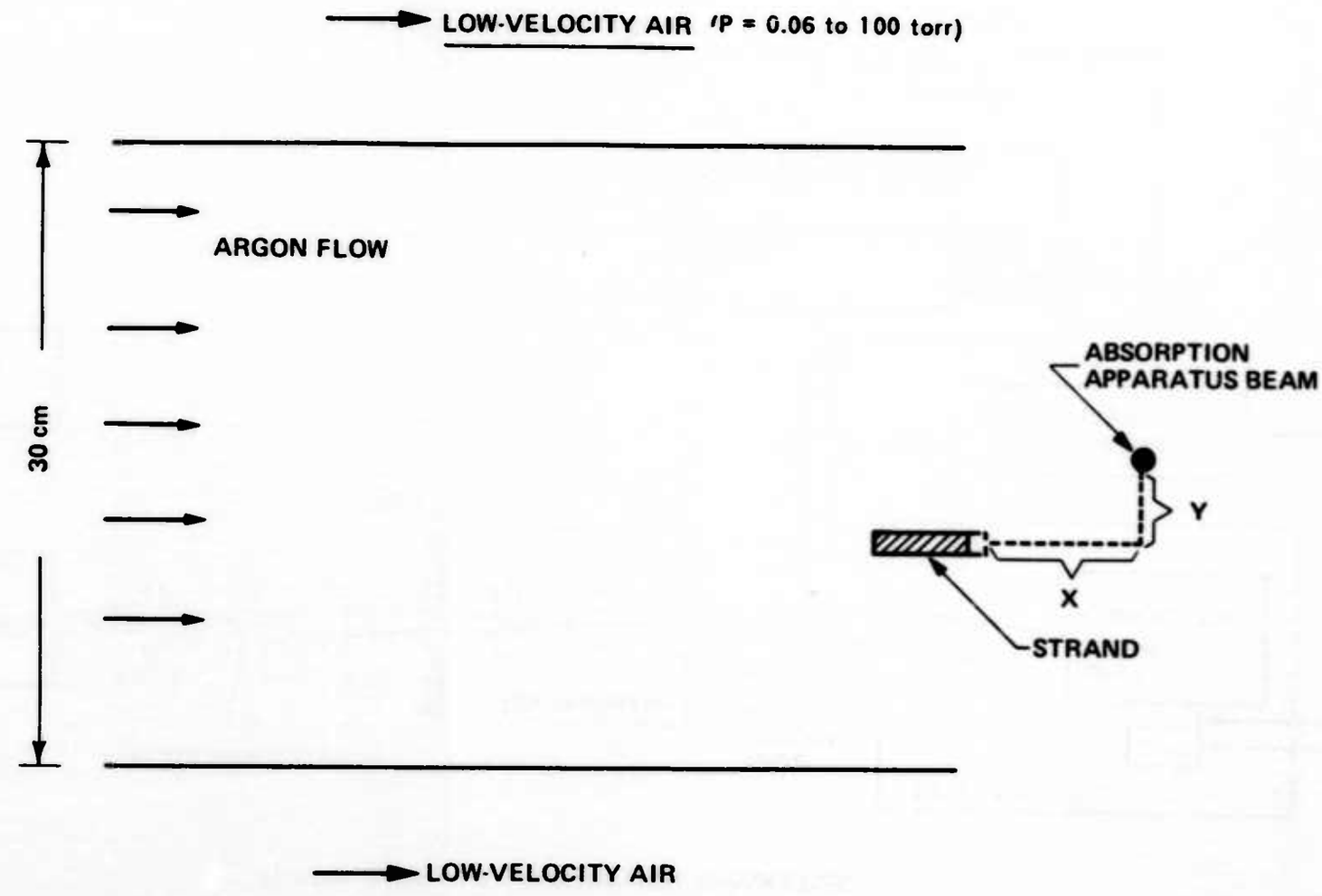

FIGURE 2. OPTICAL ABSORPTION APPARATUS.

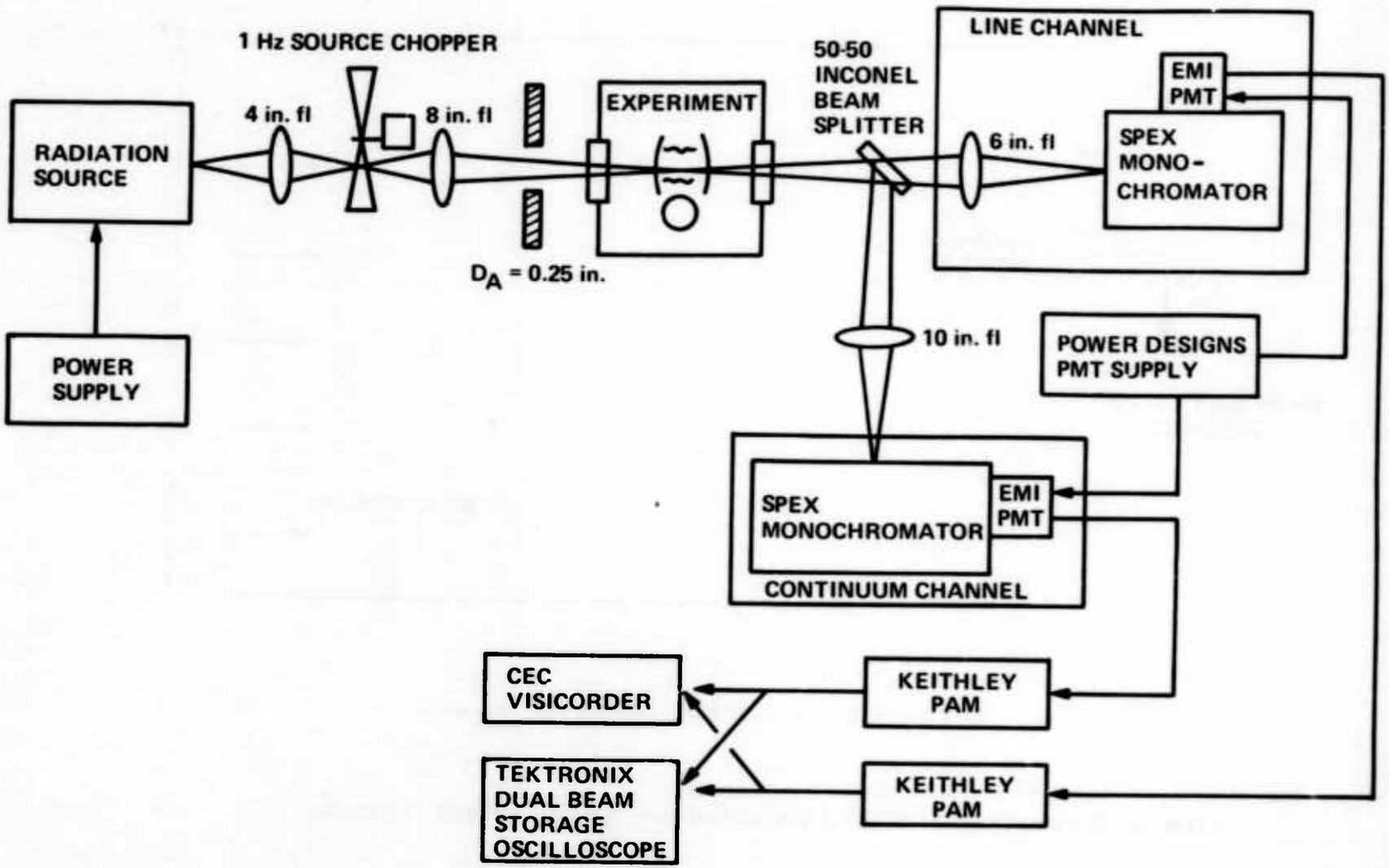

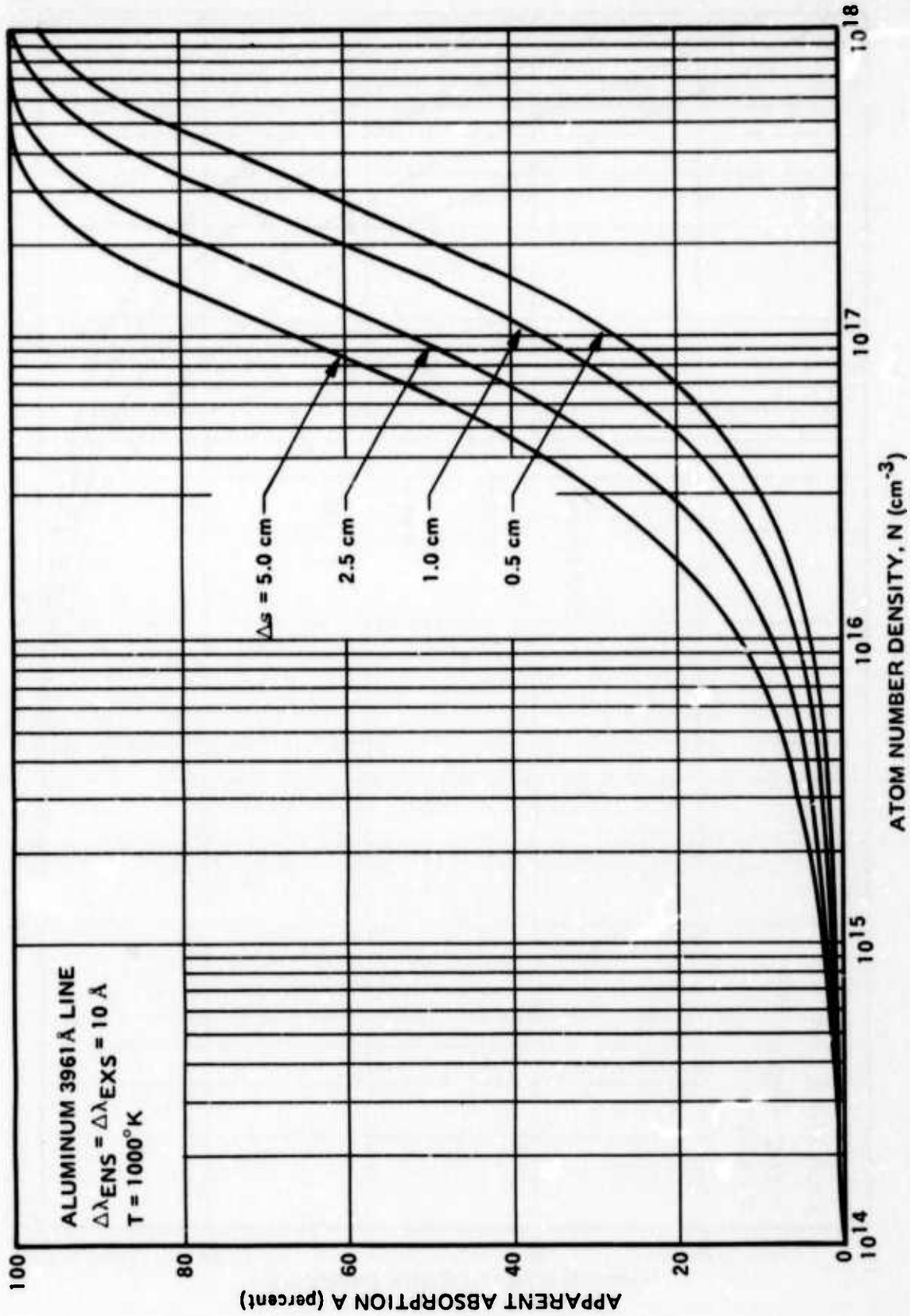

FIGURE 3. CONTINUUM SOURCE ALUMINUM MEASUREMENTS.

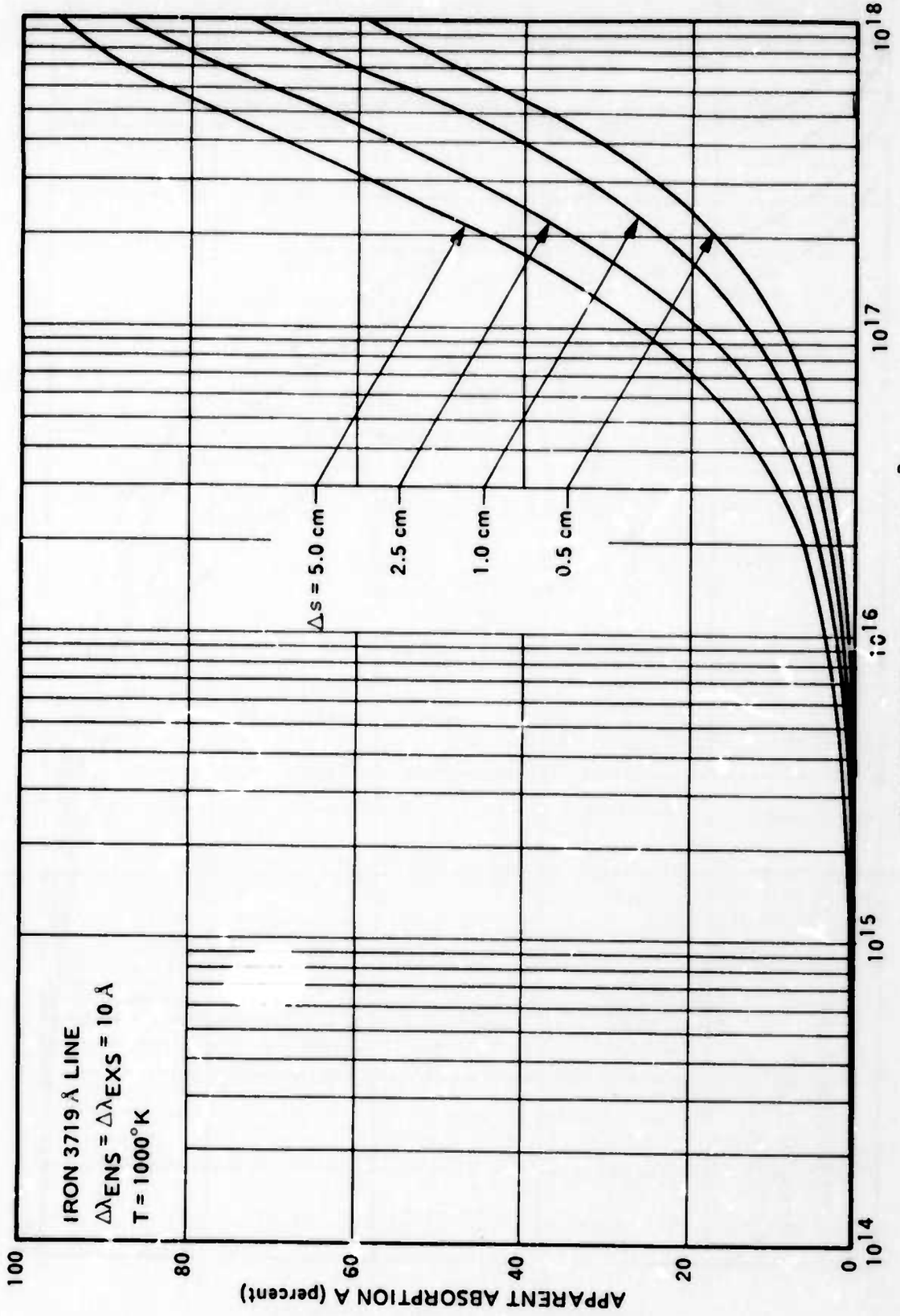

FIGURE 4. CONTINUUM SOURCE IRON MEASUREMENTS.

FIGURE 5. ALUMINUM OR IRON STRAND RELEASES.